



Butyralization of poly(vinyl alcohol) under supercritical carbon dioxide for a humidity-resistant adhesive to glass substrates

Matsumoto, Takuya
Yorifuji, Miyabi
Sugiyama, Yuya
Nishino, Takashi

(Citation)

Polymer Journal, 52(12):1349-1356

(Issue Date)

2020-12

(Resource Type)

journal article

(Version)

Accepted Manuscript

(Rights)

© 2020, The Society of Polymer Science, Japan

(URL)

<https://hdl.handle.net/20.500.14094/90007468>



Butyralization of poly(vinyl alcohol) under supercritical carbon dioxide for humid-resistant adhesive to glass substrates

*Takuya Matsumoto, Miyabi Yorifuji, Yuya Sugiyama Takashi Nishino**

Department of Chemical Science and Engineering, Graduate School of Engineering, Kobe University

Rokko, Nada, Kobe 657-8501, Japan

Keywords

poly(vinyl butyral), supercritical carbon dioxide, butyralization, acetalization, humid-resistant adhesive

ABSTRACT

Poly(vinyl butyral) (PVB) was widely accepted as an adhesives for glass substrates of the window of the automobiles. In this work, we suggested and performed butyralization of poly(vinyl alcohol) (PVA) under supercritical carbon dioxide ($sc\text{-CO}_2$) and investigated on the structure and mechanical properties of the obtained PVB as well as adhesion properties under various condition, comparing with the other PVBs prepared in the solution and swollen states. The conversion ratio of butyralization under $sc\text{-CO}_2$ was larger than that in the swollen state and lower than in the solution state, which was sufficient for the material performance as the adhesive for glass substrates. The Young's modulus and tensile strength of the PVB under $sc\text{-CO}_2$ were higher than those of the other PVBs. The mechanical properties of the PVB prepared under $sc\text{-CO}_2$ have no correlation to the modification ratios because $sc\text{-CO}_2$ penetrated into the amorphous region of PVA and modified its hydroxyl groups preferentially. Furthermore, the adhesive strengths of all the obtained PVB were increased and, under high humidity atmosphere, the adhesive strength of the PVB prepared under $sc\text{-CO}_2$ was largest. The humid-resistant performance of the PVB adhesive prepared under $sc\text{-CO}_2$ was proved.

Introduction

Poly(vinyl alcohol) (PVA) has been functionalized through their polymer reaction of its hydroxyl groups.¹⁻⁷ For example, the formalization of PVA is one of the typical post-polymerization functionalization methods and provides “vinylon” fibers industrially.⁸ In addition, poly(vinyl butyral) (PVB) is obtained through acetalization of PVA using butyl aldehyde. PVB is accepted as an adhesive for lamination of glass and as a high-barrier layer towards moisture permeation in device sealing.⁹⁻¹⁵ The adhesive properties are attributed to the polar hydroxyl groups of vinyl alcohol units and flexible moieties of butyral side chains. The moisture-sealing property is provided from the hydrophobicity of butyl side chains of PVB. Therefore, PVB is widely accepted in automotive and architectural glass as well as in encapsulation of thin film silicon solar cell modules. From these reasons, various synthesis methods of the reaction of PVA with aldehydes have been reported¹⁶⁻²⁰; for examples, precipitation, dissolution, homogenous reaction and heterogeneous reaction. In addition, direct conversion from poly(vinyl acetate) PVAc to poly(vinyl acetal) has been also suggested. Their different mechanical performance and chemical properties depended on these various reaction methods as well as the degree of hydrolysis of PVA, and its molecular weight.

Recently, synthesis and chemical modification without volatile organic solvents have gathered much attention responding to environmental issues. Although solid state reaction and gas phase reaction have been developed, their methods have large disadvantages; poor dispersibility of substances, low penetrability into solid substrates and limitation of reactants.²¹ Supercritical fluids is one of the typical candidates as a medium in the non-organic-solvent synthesis methods because supercritical fluids possess both high diffusivity of gas and density of liquid.^{22,23} In particular, supercritical carbon dioxide (*sc*-CO₂) has not only those attractive properties as a reaction medium

but also its mild condition at the supercritical point ($T_c=31.3\text{ }^\circ\text{C}$, $P_c=7.38\text{ MPa}$), nontoxicity, high permeability and chemical inertness. In addition, pure products are obtained without removing solvent media such as vacuuming and filtering.²²⁻²⁵ From these reason, various industrial processes using *sc*-CO₂ such as extraction, dyeing, foaming and organic/polymer reaction have been reported.²⁶⁻²⁹ Therefore, we also previously have reported on modification of cellulose using *sc*-CO₂.²⁹ Homogeneous chemical modification of bulk cellulose is a challenge because of the low solubility of cellulose. We achieved the complete acetylation of cellulose in solid states under *sc*-CO₂ with its high permeability into cellulose and high solubility of the reaction reagents.

Herein, we focused on butylated PVA in the solid film state under *sc*-CO₂, investigated on its structure and evaluated its adhesion properties. The synthesized PVB under *sc*-CO₂ would be gained without any complicated purification process. Our employed acetalization of PVA under *sc*-CO₂ are expected to provide the thermal- and humid-resistance to the adhesion properties of the obtained PVB. PVB which was prepared with acetalization of PVA in the solution state was softened at higher temperature than glass transition one because of the butyl side chains. Swollen-acetalized PVA, which was prepared from swollen PVA in butyl aldehyde aqueous solution, was deteriorated mechanically by the soft butyl side chains and received the effect of moisture with the residual hydroxyl groups. In contrast, PVB modified under *sc*-CO₂ possesses 1,3-dioxane rings in the bulk and remains rigid assemble structure of PVA because of the acetalization in solid states. These would prevent the penetration of moisture and thermal molecular dynamic behavior and they led to high adhesion strength under high humidity atmosphere.

Materials and Methods

Materials

PVA (Gohsenol NH-18) was provided from Mitsubishi Chemical Co. Ltd. The degree of saponification of PVA was more than 99%. Butyl aldehyde, hydrochloric acid and dimethyl sulfoxide were purchased from Tokyo Chemical Industry Co. Ltd and Nakarai Tesque Co. Ltd. Liquefied carbon dioxide was purchased from Kobe-Sanso Co., Ltd. Deionized water was prepared with Elix[®] water purification system (Merck Millipore Co., Ltd., Elix Essential 3).

Acetalization under *sc*-CO₂

PVA 5 wt% aqueous solution (8 mL) was poured into glass dish and casted for 7 days at atmosphere. PVA cast film was dried at 60 °C under vacuum for 2 days and annealed in dry oven at 130 °C for 30 min. Thicknesses of the PVA films were about 100 μm and these films were used in acetalization using butyl aldehyde under *sc*-CO₂ and in swollen state. The PVA film was trimmed into 30 mm × 80 mm and set into a high pressure cell fixed to Teflon holder, as shown in Figure S1 in the Supporting Information. Then, butyl aldehyde (1.0 mL), and 10 M hydrochloric acid (0.2 mL) were added into the cell. After the addition, CO₂ liquid was charged into the cell with high pressure pump under heating at 60 °C and the pressure in the cell reached 15 MPa. After reaction at 60 °C for 1 h, the cell was cooled to room temperature and CO₂ in the cell was removed by reducing its pressure. The butylated PVA film was washed by deionized water. Then, film was dried at 60 °C for 24 hours. The *sc*-PVB was obtained.

Acetalization of PVA film in swollen state

Dried and annealed PVA film was immersed into aqueous solution including butyl aldehyde (5.0 mL), 10 M hydrochloric acid (1.0 mL), and distilled water (200 mL) and acetalization was

carried out at 60 °C for 1 hour in the film state. After reaction, the PVA acetalized in swollen state (*swollen*-PVB) film was washed by deionized water and dried at 60 °C for 24 hours.

Acetalization in solution

PVA powder (2.5 g) was dissolved in dimethyl sulfoxide (DMSO) (50 mL) and acetalization of PVA was carried out at 60 °C for 1 hour with butyl aldehyde (5.0 mL) and 10 M hydrochloric acid (0.5 mL). After reaction, polymer solution was poured into deionized water and precipitated of PVBs. PVBs were washed by distilled water and dried at 60 °C under vacuum for 24 hours. The yield was 12%. The *soln*-PVB was dissolved in tetrahydrofuran and casted in room temperature. After drying, the thickness of the *soln*-PVB was around 100 μm.

Nuclear magnetic resonance (NMR) measurements

¹H NMR measurements of PVA and obtained PVBs were performed with NMR spectrometer (JEOL Ltd., JNS ECZS). NMR samples were prepared as deuterated dimethyl sulfoxide (DMSO-*d*₆) solution. The frequencies of ¹H measurements were 400 MHz.

The modification ratios of the obtained PVBs were calculated from the integral ratios of the NMR peaks at 0.70-0.91 ppm from methyl *CH*₃ units and 0.92-1.62 ppm from methylene *CH*₂ units using the following equations.

$$X_{VB} (mol\%) = \frac{2}{\left(3A_{CH_2}/A_{CH_3}\right) - 6} \times 100$$

$$Acetalization\ degree\ (mol\%) = \frac{2X_{VB}}{2X_{VB} + X_{OH}} \times 100$$

where *X*_{VB} is a molar ratio of vinyl butyral groups in PVB, *X*_{OH} is that of vinyl alcohol groups, and *A*_{CH₂} and *A*_{CH₃} are integrated values of methylene *CH*₂ and methyl *CH*₃ units, respectively.

PVA

^1H NMR (400 MHz, DMSO- d_6 , δ /ppm): 1.00-1.67 (br, 2.0H, $-\text{CH}_2-\text{CH}(\text{OH})-$); 1.86-1.96 (br, 0.016H, $-\text{OCOC}\underline{\text{H}}_3$, unsaponified acetyl groups of PVA); 3.64-3.91 (br, 1.0H, $-\text{CH}_2-\text{CH}(\text{OH})-$); 4.14-4.72 (br, 1.0H, OH)

sc-PVB

^1H NMR (400 MHz, DMSO- d_6 , δ /ppm): 0.73-0.91 (br, 3.0H, $-\text{CH}_2-\text{CH}_2-\text{CH}_3$, PVB); 0.94-1.22, 1.51-1.62 (br, 5.4H, $-\text{CH}(\text{O})-\text{CH}_2-\text{CH}(\text{O})-$, PVB); 1.16-1.36 (br, 2.0H, $-\text{CH}_2-\text{CH}_2-\text{CH}_3$, PVB); 1.36-1.51 (br, 1.9H, $-\text{CH}_2-\text{CH}_2-\text{CH}_3$, PVB); 1.86-1.95 (br, 0.052H, $-\text{OCOC}\underline{\text{H}}_3$, unsaponified acetyl groups of PVA); 3.54-3.97 (br, 1.8H, $-\text{CH}_2-\text{CH}(\text{O})-\text{CH}_2-$); 4.05-4.36 (br, 0.36H, $-\text{OH}$); 4.33-4.53, 4.57-4.75 (br, 1.0H, $-\text{O}-\text{CH}(\text{C}_3\text{H}_7)-\text{O}-$, PVB)

swollen-PVB

^1H NMR (400 MHz, DMSO- d_6 , δ /ppm): 0.74-0.89 (br, 3.0H, $-\text{CH}_2-\text{CH}_2-\text{CH}_3$, PVB); 0.92-1.18, 1.51-1.62 (br, 5.8H, $-\text{CH}(\text{O})-\text{CH}_2-\text{CH}(\text{O})-$, PVB); 1.16-1.36 (br, 2.1H, $-\text{CH}_2-\text{CH}_2-\text{CH}_3$, PVB); 1.36-1.51 (br, 2.0H, $-\text{CH}_2-\text{CH}_2-\text{CH}_3$, PVB); 1.87-1.95 (br, 0.087H, $-\text{OCOC}\underline{\text{H}}_3$, unsaponified acetyl groups of PVA); 3.49-3.98 (br, 2.1H, $-\text{CH}_2-\text{CH}(\text{O})-\text{CH}_2-$); 4.01-4.33 (br, 0.60H, $-\text{OH}$); 4.37-4.52, 4.64-4.75 (br, 1.0H, $-\text{O}-\text{CH}(\text{C}_3\text{H}_7)-\text{O}-$, PVB)

soln-PVB

^1H NMR (400 MHz, DMSO- d_6 , δ /ppm): 0.70-0.88 (br, 3H, $-\text{CH}_2-\text{CH}_2-\text{CH}_3$, PVB); 0.92-1.22, 1.51-1.60 (br, 4.9H, $-\text{CH}(\text{O})-\text{CH}_2-\text{CH}(\text{O})-$, PVB); 1.16-1.34 (br, 2.0H, $-\text{CH}_2-\text{CH}_2-\text{CH}_3$, PVB); 1.34-1.51 (br, 2.0H, $-\text{CH}_2-\text{CH}_2-\text{CH}_3$, PVB); 1.85-1.95 (br, 0.057H, $-\text{OCOC}\underline{\text{H}}_3$, unsaponified acetyl groups of PVA); 3.48-3.98 (br, 1.4H, $-\text{CH}_2-\text{CH}(\text{O})-\text{CH}_2-$); 4.04-4.20 (br, 0.16H, $-\text{OH}$); 4.33-4.53, 4.62-4.75 (br, 1.0H, $-\text{O}-\text{CH}(\text{C}_3\text{H}_7)-\text{O}-$, PVB)

Fourier-transform infrared (FTIR) spectroscopy

FTIR spectroscopy was performed with IRTracer-100 (Shimadzu). The measured samples were dispersed in KBr pellets. For the measurement of only the surface of the samples, attenuated total reflection (ATR)-FTIR was carried out by AIM-9000 (Shimadzu) using a Ge crystal. The resolution of wavenumber was 4 cm^{-1} , and the accumulation number was 20.

Raman scattering spectroscopy

Raman scattering spectroscopy with line scanning mode was performed using confocal Raman scattering microscope alpha 300R (WITech Co. Ltd.). The cross sections of *sc*-PVB and *swollen*-PVB were exposed with a razor and were measured in the direction parallel to the thickness from the surface, as shown in Figure S2 in the Supporting Information. The wavelength of laser was 532 nm (ND/YAG laser) and the step distance was around 300 nm/step. The intensity ratio I_{2882}/I_{2933} of Raman bands at 2882 cm^{-1} and 2933 cm^{-1} were plotted along the line-scanning position.

X-ray diffraction (XRD) measurements

XRD measurements of the prepared PVA and PVB films were performed with RINT2000 in $\theta/2\theta$ reflection method. The wavelength of the X-ray beam was 1.5418 \AA ($\text{CuK}\alpha$). The scanning rate was $2^\circ/\text{min}$ and the scanning angle 2θ was from 5° to 40° .

Thermal properties of PVA and PVB

Decomposition temperature was measured with a thermogravimetric analysis (TGA) instrument Thermo plus EVO2: TG8121 (Rigaku) using Al pans. The measurement temperature was from room temperature (about $24\text{ }^\circ\text{C}$) to $400\text{ }^\circ\text{C}$. The heating speed was $10\text{ }^\circ\text{C}/\text{min}$. The temperature where 5 wt% samples were lost was defined as a decomposition temperature T_{5d} .

Differential scanning calorimetry (DSC) measurements of PVA and PVB were performed with Thermo plus EVO II: DSC8230 (Rigaku) using Al pans. The measurement temperature was from $-100\text{ }^\circ\text{C}$ to $250\text{ }^\circ\text{C}$. The heating speed was $10\text{ }^\circ\text{C}/\text{min}$.

Measurements of dynamic contact angles of water and methylene iodide droplets on surface of PVA and PVB films and calculation of their surface free energies

Advancing and receding contact angles (θ_a and θ_r) of water and methylene iodide droplets on surface of the prepared polymer films were observed with optical microscopy OL-35 (HIROX). From their dynamic contact angles, the averaged contact angles θ were calculated as follows;

$$\cos \theta_{av} = \frac{\cos \theta_a + \cos \theta_r}{2}$$

Surface free energies γ_S of their polymers were calculated using the following Young-Owens equation.³⁰

$$\frac{(1 + \cos\theta)\gamma_L}{2} = \sqrt{\gamma_S^d \gamma_L^d} + \sqrt{\gamma_S^p \gamma_L^p}$$

$$\gamma_X = \gamma_X^d + \gamma_X^p$$

$$(X = S \text{ or } L)$$

where γ_L was surface free energies of droplet liquid, and γ_X^d and γ_X^p were dispersion and polar components of the surface free energies of substrate polymer ($X = S$) or liquid solvent ($X = L$). In addition, γ_L^d and γ_L^p of water and methylene iodide were $\gamma_{\text{water}}^d = 21.8 \text{ mJ/m}^2$ and $\gamma_{\text{water}}^p = 51.8 \text{ mJ/m}^2$, and $\gamma_{\text{CH}_2\text{I}_2}^d = 48.5 \text{ mJ/m}^2$ and $\gamma_{\text{CH}_2\text{I}_2}^p = 2.3 \text{ mJ/m}^2$, respectively.³¹

Tensile tests of PVA and PVBs

Tensile tests were carried out with a tensile tester autograph AG-X plus (Shimadzu). The samples were trimmed into 40 mm \times 5 mm. The tensile rate was 5 mm/min. The initial length was 20 mm. For the reliable data, we performed tensile tests of more than five specimens every sample, and averaged their measurement values.

Lap shear joint tests

We prepared adhered specimens for lap shear joint tests. PVA or PVB films were sandwiched with two slide glass substrates (76 mm × 26 mm × 1.5 mm) and hot-pressed at 2 MPa and 140 °C for 5 min. The adhered areas were 10 mm × 10 mm. The thickness of the adhesive layer was around 100 μm. For adhesion tests under high humidity, the specimens were stored at 40 °C for 12 h before the lap shear joint tests.

The lap shear joint tests were performed with autograph AG-X plus (Shimadzu). The shear rate was 50 mm/min. The shear tests were carried out under ambient, high-temperature (80 °C) and high-humidity (40 °C and 80 %RH) atmosphere. For the reliable data, we performed lap shear joint tests of more than five specimens every sample under each condition, and averaged their obtained lap shear strengths.

Swelling tests

Swelling tests of PVA and obtained PVBs were carried out using their film samples trimmed into approximately 7 mm × 7 mm. We compared the size and weight of the film samples before and after immersed into water at room temperature for 2 hours.

Results and discussion

We prepared PVB through three types of butyralization with PVA. Their NMR charts and IR spectra were shown in Figure S3 in the Supporting Information and Figure 1. First, in the acetalization using butyl aldehyde in solution states, PVA was dissolved into DMSO and the butyralization to hydroxyl groups of PVA progressed homogeneously and the randomly acetalized PVB was obtained. From the peaks at 0.92-1.22 ppm and 1.51-1.60 ppm in the NMR chart, it is revealed that the 1,3-dioxane units were formed.³² In the FTIR spectrum as shown in Figure 1a, the absorption bands of hydroxyl vibration were decreased at 3468 cm^{-1} and the vibration bands of ether units appeared at 1140 cm^{-1} .³³ The degree of acetalization was 81%. Second, for the butyralization of PVA in the swollen state, the PVA films were immersed into butyl aldehyde aqueous solution, then the reaction with butyl aldehyde was performed involving the penetration of the reagents. Actually, the NMR chart of *swollen*-PVB showed peaks of PVA and PVB. In addition, in the IR spectrum in a KBr pellet as shown in Figure 1a, the vibration bands of hydroxyl groups also remained and that of ether units was observed, while, in the ATR-FTIR spectrum in Figure 1b, the band of hydroxyl group was reduced and the band of the ether group was increased relatively. The degree of acetalization of *swollen*-PVB was 66%. Third, for the acetalization of the PVA films using butyl aldehyde under *sc*-CO₂, the high permeability and high solubility of *sc*-CO₂ led to butyralization not only at the surface but also in the bulk. The NMR chart of *sc*-PVB showed peaks of 1,3-dioxane moieties at 0.94-1.12 ppm and 1.51-1.62 ppm and the IR spectra in both the transmission and ATR mode represented the decrease of hydroxyl groups and the observation of vibration bands of ether units. The degree of acetalization was calculated as 75%.

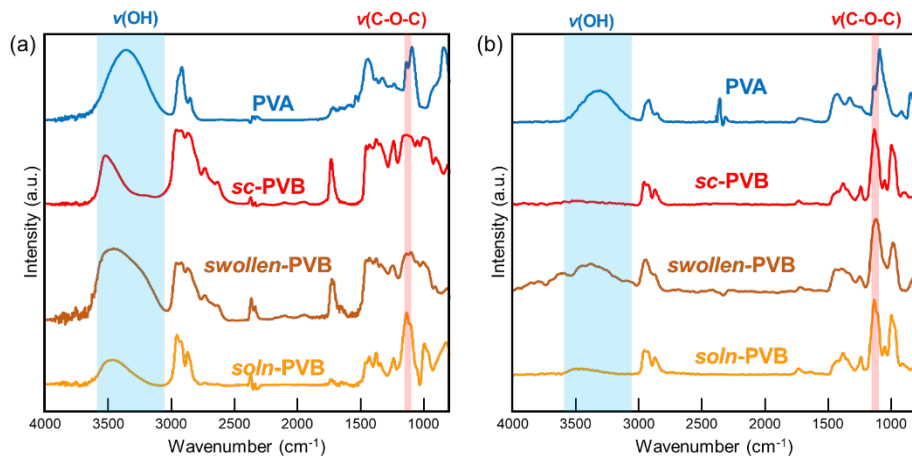


Figure 1. FT-IR spectra of PVA, *sc*-PVB, *swollen*-PVB and *soln*-PVB films by (a) transmission method and (b) ATR method.

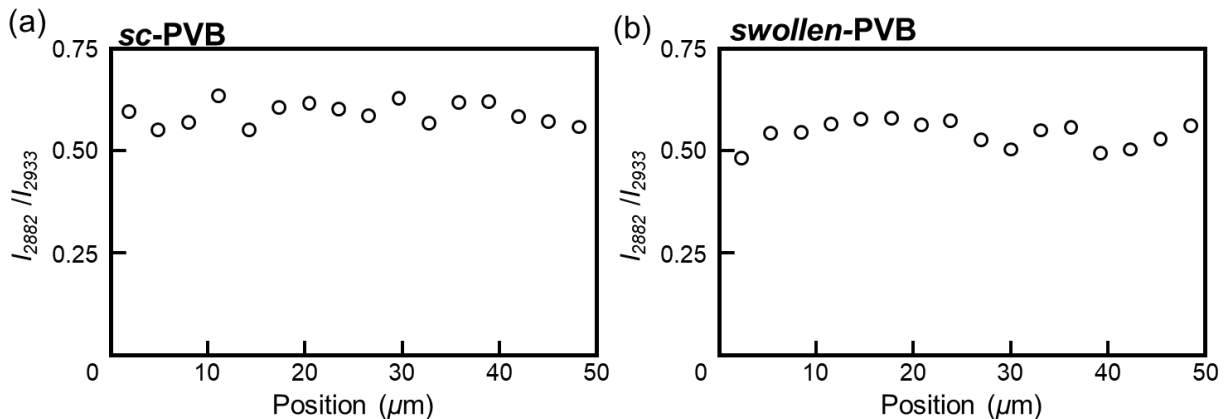


Figure 2. Intensity ratios of Raman bands at 2882 cm^{-1} and 2933 cm^{-1} of cross section of (a) *sc*-PVB, and (b) *swollen*-PVB films in the direction perpendicular to the surface.

In order to evaluate on the regions modified with butyl aldehyde, Raman scattering spectra of the cross sections of *sc*-PVB and *swollen*-PVB were measured in the line scanning mode with a confocal Raman microscope. The measurements were performed from the surface side in the direction perpendicular to the surface and the Raman band intensity ratios I_{2882}/I_{2933} at 2882 cm^{-1}

and 2933 cm^{-1} were plotted at all the position, as shown in Figure 2. These Raman bands were originated from the C–H vibration of alkyl units.³⁴ The intensity ratios in both PVB films had no change. This result means that the butyl aldehyde reagent penetrated into the PVA films through *sc*-CO₂ and aqueous solution and both the prepared PVB films were modified not only at surface but also in the bulk.

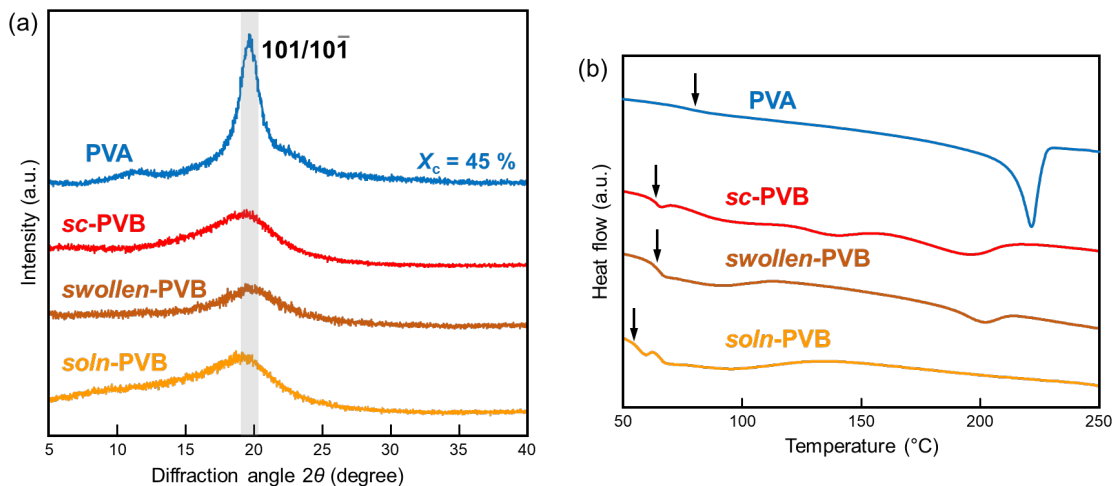


Figure 3. (a) X-ray diffraction profiles and (b) DSC thermograms of PVA, *sc*-PVB, *swollen*-PVB and *soln*-PVB films. The glass transition in the DSC thermograms were points with arrows.

For the investigation on crystalline structures and crystallinities of the prepared PVBs, X-ray diffraction measurements were performed. Figure 3a shows X-ray diffraction profiles of PVA, *sc*-PVB, *swollen*-PVB and *soln*-PVB. In the PVB films, the diffraction peak originated from (101)/(10-1) lattice planes of PVA crystallites at 19.7° disappeared and only the amorphous halo was observed. Even the *swollen*-PVB and *sc*-PVB films possessed no crystalline structure. The swollen state modification of conventional crystalline polymers have been reported by Moore and co-workers.^{35–38} In the case of *syndiotactic* polystyrene and poly(ether ether ketone), after modification in swollen states, some parts of crystallite regions were remained. In contrast, the

acetalization of PVA with butyl aldehyde in swollen state disappeared their crystalline structure. The intra- and intermolecular acetalization involving two hydroxyl groups of PVA would provide destruction of the crystallites. The amorphous structure of butyral units was also observed with their DSC thermograms as shown in Figure 3b. The melting peaks of PVA at 225 °C was not clearly observed in the DSC thermograms of all the PVB films, but the glass transitions of all the PVBs were appeared at around 60 °C³⁹ and the broad endothermic peaks in the DSC curves of *sc*-PVB and *swollen*-PVB were observed at around 200 °C. These broad endothermic peaks might be attributed to the residual crystallite regions with small sizes or crystallite-like amorphous regions with chain conformation similar to the crystallite region of PVA.

The acetalization using butyl aldehyde have effects of the surface properties. Their contact angles and surface free energies were shown in Table 1. All the acetalization methods led to the hydrophobicity of the surface. These results mean that the hydrophilic hydroxyl groups of PVA were reacted with butyl aldehyde and were changed to 1,3-dioxane units. In the *sc*-PVB and *swollen*-PVB, their surface free energies were decreased with acetalization. In addition, *sc*-PVB and *swollen*-PVB possessed 25% and 34% of the PVA units, more than *soln*-PVB, respectively, while their surface free energies were compared with that of *soln*-PVB. These results suggested that, at the top surface of not only *swollen*-PVB but also the *sc*-PVB films, the acetalization was progressed more preferentially than in their bulk. These were coincidence with the results from their ATR-FTIR measurements.

Table 1. Contact angles and surface free energies γ of PVA, *sc*-PVB, *swollen*-PVB and *soln*-PVB films.

Sample	Water	Methylene iodide	Surface free energy
	Degree ($\theta_a / \theta_r / \theta_{av}$)		mJ/m ² ($\gamma / \gamma^p / \gamma^d$)
PVA	54.5±2.4 / 26.9±4.3 /	46.0±2.4 / 28.7±1.1 /	57.3 / 28.7 / 28.6
	42.6±2.7	38.2±1.3	
<i>sc</i> -PVB	91.2±3.0 / 59.7±4.0 /	74.0±4.2 / 46.4±7.5 /	32.7 / 10.6 / 22.0
	76.0±1.9	61.2±3.3	
<i>swollen</i> -PVB	96.2±1.8 / 35.6±3.6 /	64.0±5.1 / 33.4±4.2 /	39.3 / 12.2 / 27.1
	69.4±1.8	50.5±3.8	
<i>soln</i> -PVB	90.8±1.1 / 37.3±12.1 /	61.1±2.7 / 27.6±1.2 /	41.6 / 12.9 / 28.8
	67.4±4.3	46.8±1.3	

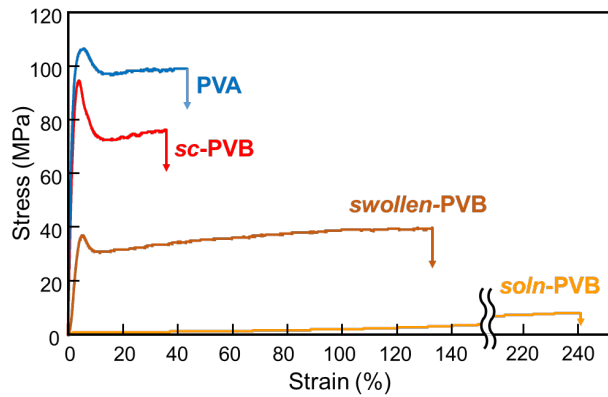


Figure 4. Stress-strain curves of PVA, *sc*-PVB, *swollen*-PVB and *soln*-PVB films.

As shown in Figure 4 and Table S3 in the Supporting Information, their Young's modulus and tensile tests of *soln*-PVB, *swollen*-PVB, *sc*-PVB and PVA were increased in this order. This reason was not only the fraction ratios of unmodified vinyl alcohol units. It is said that these mechanical properties of PVBs were provided from butyl groups of PVB after butyralization.⁴⁰ Because the crystallite regions were disappeared and the hydrogen bonding of the hydroxyl groups of PVA reduced, the modulus of all the obtained PVB were lower than that of PVA. In this study, the larger modulus and strength of *sc*-PVB would be attributed to the chain conformation in the crystallite regions of PVA before modification, in the *sc*-PVB. In contrast, *soln*-PVB with the largest fraction of butyl units possessed the highest elongation at break and *swollen*-PVB was the second.

We investigated effects of acetalization using butyl aldehyde on adhesion properties to glass substrates through lap shear joint tests. Figure 5 shows the lap shear strength of adhered samples using PVA and modified PVBs under (a) ambient, (b) high temperature and (c) high humidity atmosphere. The lap shear strength under ambient atmosphere was increased with acetalization of PVA using butyl aldehyde through any methods.^{9,12} The adhered samples with PVA were failed at interface between glass substrate and PVA. In contrast, the lap shear joint samples of all the modified PVBs was fractured at their glass substrates. In the lap shear joint tests under high temperature 80 °C, the adhesive strengths of all the samples were decreased relative to those under ambient atmosphere and the interfacial peeling was observed at the fracture. This measurement temperature was higher than the glass transition temperature of PVA and the obtained PVB. At the higher temperature than glass transition temperature, the molecular mobility was increased and the polymer materials were softened. This is the reason for the decrease of lap shear strength at high temperature atmosphere. Furthermore, under high humidity atmosphere, the adhesive strengths of the samples adhered with PVA and *swollen*-PVB were not able to be measured because the adhered

samples were peeled when these were set on the tensile machine. This reason is that vinyl alcohol units possessed high affinities to hydroxyl groups and these adhesives absorbed water. In the case of *soln*-PVB, the lap shear strength was decreased relative to that under ambient atmosphere, but the adhesive strength under high humidity atmosphere was larger than those of PVA and *swollen*-PVB. The high modification ratio of *soln*-PVB would prevent its water absorption. In contrast, the shear strength of *sc*-PVB under high humidity atmosphere kept higher compared with that under ambient atmosphere. This high strength was attributed to the higher Young's modulus and higher tensile strength and the more hydrophobicity of *sc*-PVB compared with those of others. These results that *sc*-PVB possessed high performance as a water-resistant adhesive for glass substrates.

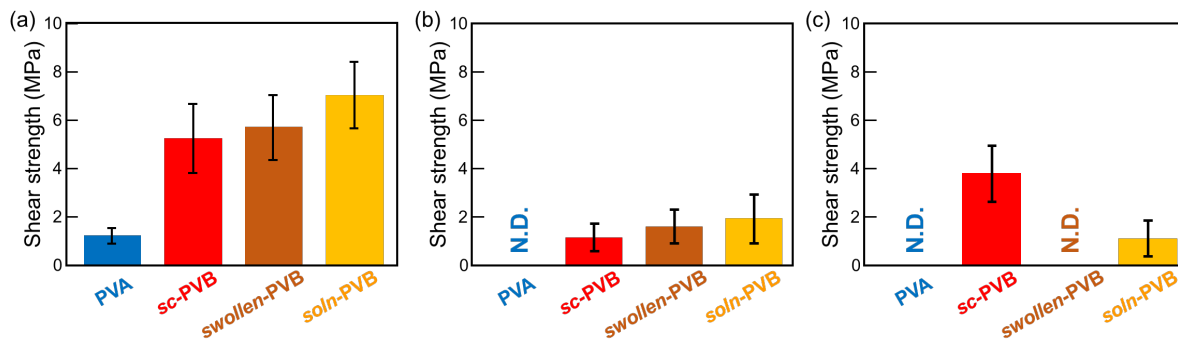


Figure 5. Lap shear strength of PVA, *sc*-PVB, *swollen*-PVB and *soln*-PVB films (a) at room temperature, (b) at 80 °C, and (c) at 40 °C and 80 %RH.

Conclusions

We demonstrated butyralization of poly(vinyl alcohol) under supercritical carbon dioxide medium and investigated on the structure and physical properties of the obtained poly(vinyl butyral). The butyralization under supercritical carbon dioxide were progressed not only at the

surface but also in the bulk and the high conversion efficiency was achieved sufficiently. The Young's modulus and tensile strength of the poly(vinyl butyral) under supercritical carbon dioxide were higher regardless of conversion ratios. These properties were attributed to the preferential permeation of carbon dioxide, which penetrates and modifies amorphous region, not crystalline region, in crystalline polymers preferentially. In the investigation on the adhesive property for glass substrates, the large lap shear strength of the poly(vinyl butyral) under supercritical carbon dioxide was observed compared with the other poly(vinyl butyral). In addition, even under high humidity atmosphere, the lap shear strength of only the poly(vinyl butyral) under supercritical carbon dioxide was kept remained. The adhesive of poly(vinyl butyral) under supercritical carbon dioxide possessed humid resistance. The butyralization of poly(vinyl alcohol) with butyl aldehyde under supercritical carbon dioxide medium was a promising method for the preparation of the advanced materials.

ASSOCIATED CONTENT

Supplementary data.

Reaction system of acetalization under *sc*-CO₂, Raman scattering spectra, ¹H NMR spectra, acetalization degree, thermogravimetric trace curves, thermal properties, mechanical properties are described in the Supporting Information.

AUTHOR INFORMATION

Corresponding Author

*(T.N.) E-mail: tnishino@kobe-u.ac.jp

ACKNOWLEDGEMENTS

This work was supported by JSPS KAKENHI Grant Number JP12345678.

Notes

The authors declare no competing financial interest.

REFERENCES

1. Delattre, E., Lemière, G., Desmurs, J.-R., Boulay, B. & Duñach, E. Poly(vinyl alcohol) functionalization with aldehydes in organic solvents: Shining properties of poly(vinyl acetals). *J. Appl. Polym. Sci.* **131**, 40677 (2014).
2. Giménez, V., Mantecón, A. & Cádiz, V. Modification of poly(vinyl alcohol) with acid chlorides and crosslinking with difunctional hardeners. *J. Polym. Sci. Part A Polym. Chem.* **34**, 925–934 (1996).
3. Flory, P. J. Intramolecular Reaction between Neighboring Substituents of Vinyl Polymers. *J. Am. Chem. Soc.* **61**, 1518–1521 (1939).
4. Gaina, C., Gaina, V. & Ionita, D. Functional modification of poly(vinyl alcohol) with maleimide compounds. *Polym. Bull.* **73**, 2019–2038 (2016).
5. Zhao, B., Lu, C. H. & Liang, M. Solvent-free esterification of poly(vinyl alcohol) and maleic anhydride through mechanochemical reaction. *Chinese Chem. Lett.* **18**, 1353–1356 (2007).
6. Anbarasan, R., Pandiarajaguru, R., Prabhu, R., Dhanalakshmi, V., Jayalakshmi, A., Dhanalakshmi, B., Nisha, S. U., Gandhi, S. & Jayalakshmi, T. Synthesis, characterizations, and mechanical properties of structurally modified poly(vinyl alcohol). *J. Appl. Polym. Sci.* **117**, 2059–2068 (2010).
7. Gaina, C., Ursache, O., Gaina, V. & Ionita, D. Study on the Chemical Modification of Poly(Vinyl Alcohol) with 4-Maleimidophenyl Isocyanate. *Polym. Plast. Technol. Eng.* **51**, 65–70 (2012).

8. Sakurada, I. in *Polyvinyl Alcohol Fibers* 211–230 (Marcel Dekker, Inc., 1985).
9. Nguyen, F. N. & Berg, J. C. The effect of vinyl alcohol content on adhesion performance in poly(vinyl butyral)/glass systems. *J. Adhes. Sci. Technol.* **18**, 1011–1026 (2004).
10. Chen, W., David, D. J., MacKnight, W. J. & Karasz, F. E. Miscibility and Phase Behavior in Blends of Poly(vinyl butyral) and Poly(methyl methacrylate). *Macromolecules* **34**, 4277–4284 (2001).
11. Elzière, P., Fourton, P., Demassieux, Q., Chennevière, A., Dalle-Ferrier, C., Creton, C., Ciccotti, M. & Barthel, E. Supramolecular Structure for Large Strain Dissipation and Outstanding Impact Resistance in Polyvinylbutyral. *Macromolecules* **52**, 7821–7830 (2019).
12. Huntsberger, J. R. Adhesion of Plasticized Polyvinyl Butyral) to Glass. *J. Adhes.* **13**, 107–129 (1981).
13. Zhu, G., Cui, X., Zhang, Y., Chen, S., Dong, M., Liu, H., Shao, Q., Ding, T., Wu, S. & Guo, Z. Poly (vinyl butyral)/Graphene oxide/poly (methylhydrosiloxane) nanocomposite coating for improved aluminum alloy anticorrosion. *Polymer* **172**, 415–422 (2019).
14. Tsugawa, N., Ito, A. & Yamaguchi, M. Effect of lithium salt addition on the structure and optical properties of PMMA/PVB blends. *Polymer* **146**, 242–248 (2018).
15. Pizzanelli, S., Prevosto, D., Labardi, M., Guazzini, T., Bronco, S., Forte, C. & Calucci, L. Dynamics of poly(vinyl butyral) studied using dielectric spectroscopy and ¹H NMR relaxometry. *Phys. Chem. Chem. Phys.* **19**, 31804–31812 (2017).

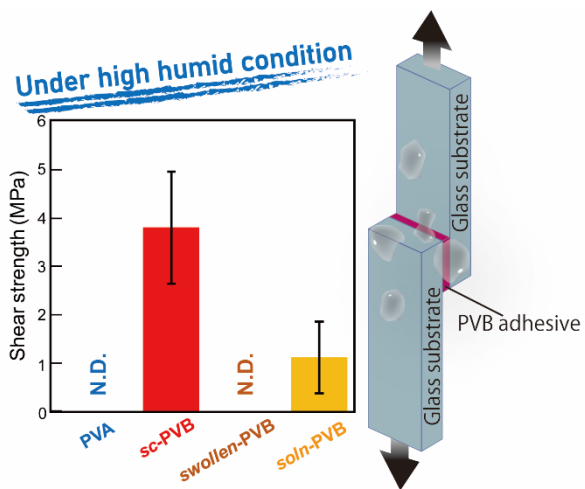
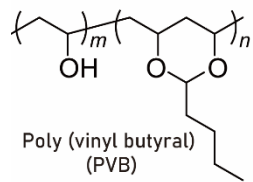
16. Yang, B., Liu, R., Huang, J. & Sun, H. Reverse Dissolution as a Route in the Synthesis of Poly(vinyl butyral) with High Butyral Contents. *Ind. Eng. Chem. Res.* **52**, 7425–7431 (2013).
17. Dasgupta, A. M., David, D. J. & Misra, A. Synthesis and characterization of ionomeric poly(vinyl butyral). *J. Appl. Polym. Sci.* **44**, 1213–1221 (1992).
18. Fernández, M. D., Fernández, M. J. & Hoces, P. Synthesis of poly(vinyl butyral)s in homogeneous phase and their thermal properties. *J. Appl. Polym. Sci.* **102**, 5007–5017 (2006).
19. Saravanan, S., Akshay Gowda, K. M., Arul Varman, K., Ramamurthy, P. C. & Madras, G. In-situ synthesized poly(vinyl butyral)/MMT-clay nanocomposites: The role of degree of acetalization and clay content on thermal, mechanical and permeability properties of PVB matrix. *Compos. Sci. Technol.* **117**, 417–427 (2015).
20. Chetri, P. & Dass, N. N. Preparation of poly(vinyl butyral) with high acetalization rate. *J. Appl. Polym. Sci.* **81**, 1182–1186 (2001).
21. Chang, B. H., Zeigler, R. & Hiltner, A. Chlorinated high density polyethylene. I. Chain characterization. *Polym. Eng. Sci.* **28**, 1167–1172 (1988).
22. Jung, J. & Perrut, M. Particle design using supercritical fluids: Literature and patent survey. *J. Supercrit. Fluids* **20**, 179–219 (2001).
23. Yeo, S.-D. & Kiran, E. Formation of polymer particles with supercritical fluids: A review. *J. Supercrit. Fluids* **34**, 287–308 (2005).

24. Koytsoumpa, E. I., Bergins, C. & Kakaras, E. The CO₂ economy: Review of CO₂ capture and reuse technologies. *J. Supercrit. Fluids* **132**, 3–16 (2018).
25. Meziani, M. J., Pathak, P., Desai, T. & Sun, Y.-P. Supercritical Fluid Processing of Nanoscale Particles from Biodegradable and Biocompatible Polymers. *Ind. Eng. Chem. Res.* **45**, 3420–3424 (2006).
26. Lee, H., Terry, E., Zong, M., Arrowsmith, N., Perrier, S., Thurecht, K. J. & Howdle, S. M. Successful Dispersion Polymerization in Supercritical CO₂ Using Polyvinylalkylate Hydrocarbon Surfactants Synthesized and Anchored via RAFT. *J. Am. Chem. Soc.* **130**, 12242–12243 (2008).
27. Ivanovic, J., Milovanovic, S. & Zizovic, I. Utilization of supercritical CO₂ as a processing aid in setting functionality of starch-based materials. *Starch - Stärke* **68**, 821–833 (2016).
28. Yalpani, M. Supercritical fluids: puissant media for the modification of polymers and biopolymers. *Polymer* **34**, 1102–1105 (1993).
29. Nishino, T., Kotera, M., Suetsugu, M., Murakami, H. & Urushihara, Y. Acetylation of plant cellulose fiber in supercritical carbon dioxide. *Polymer* **52**, 830–836 (2011).
30. Owens, D. K. & Wendt, R. C. Estimation of the surface free energy of polymers. *J. Appl. Polym. Sci.* **13**, 1741–1747 (1969).
31. Fowkes, F. M. ATTRACTIVE FORCES AT INTERFACES. *Ind. Eng. Chem.* **56**, 40–52 (1964).
32. Bruch, M. D. & Bonesteel, J. A. K. Interpretation of the proton NMR spectrum of poly(vinyl butyral) by two-dimensional NMR. *Macromolecules* **19**, 1622–1627 (1986).

33. Liao, L. C. K., Yang, T. C. K. & Viswanath, D. S. Mechanism of degradation of poly(vinyl butyral) using thermogravimetry/fourier transform infrared spectrometry. *Polym. Eng. Sci.* **36**, 2589–2600 (1996).
34. Prosanov, I. Y. & Matvienko, A. A. Study of PVA thermal destruction by means of IR and Raman spectroscopy. *Phys. Solid State* **52**, 2203–2206 (2010).
35. Fahs, G. B., Benson, S. D. & Moore, R. B. Blocky Sulfonation of Syndiotactic Polystyrene: A Facile Route toward Tailored Ionomer Architecture via Postpolymerization Functionalization in the Gel State. *Macromolecules* **50**, 2387–2396 (2017).
36. Noble, K. F., Noble, A. M., Talley, S. J. & Moore, R. B. Blocky bromination of syndiotactic polystyrene via post-polymerization functionalization in the heterogeneous gel state. *Polym. Chem.* **9**, 5095–5106 (2018).
37. Anderson, L. J., Yuan, X., Fahs, G. B. & Moore, R. B. Blocky Ionomers via Sulfonation of Poly(ether ether ketone) in the Semicrystalline Gel State. *Macromolecules* **51**, 6226–6237 (2018).
38. Anderson, L. J. & Moore, R. B. Sulfonation of blocky brominated PEEK to prepare hydrophilic-hydrophobic blocky copolymers for efficient proton conduction. *Solid State Ionics* **336**, 47–56 (2019).
39. Parker, A. A., Hedrick, D. P. & Ritchey, W. M. Studies of thermal transition behavior in plasticized poly(vinyl butyral-co-vinyl alcohol) with solid-state NMR and thermal analysis techniques. *J. Appl. Polym. Sci.* **46**, 295–301 (1992).

40. Dhaliwal, A. K. & Hay, J. N. The characterization of polyvinyl butyral by thermal analysis. *Thermochim. Acta* **391**, 245–255 (2002).
41. Carini Jr., G., Carini, G., D'Angelo, G., Federico, M., Marco, G. Di & Bartolotta, A. Enhancing the molecular cooperativity of polyvinyl butyral using liquid additives. *J. Polym. Sci. Part B Polym. Phys.* **56**, 340–346 (2018).

Graphical abstract



Supporting Information

Butyralization of poly(vinyl alcohol) under supercritical carbon dioxide for a humidity-resistant adhesive to glass substrates

*Takuya Matsumoto, Miyabi Yorifuji, Yuya Sugiyama, Takashi Nishino**

Department of Chemical Science and Engineering, Graduate School of Engineering,
Kobe University, Rokko, Nada, Kobe, 657-8501, Japan.

E-mail: tnishino@kobe-u.ac.jp

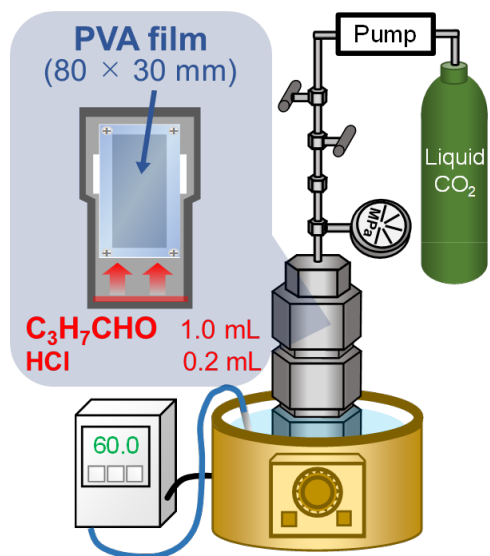


Figure S1. Reaction system of acetalization under *sc*-CO₂.

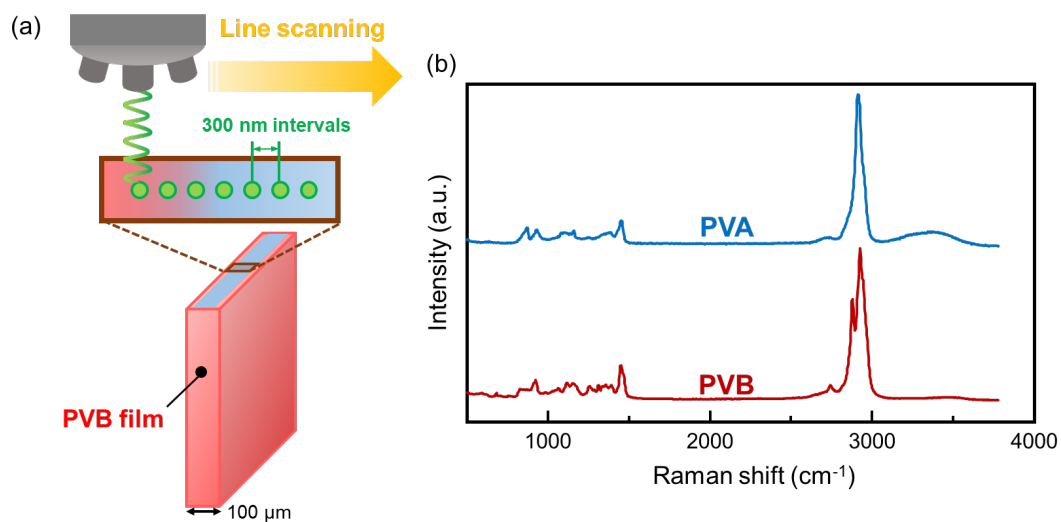


Figure S2. (a) Geometry of Raman scattering measurements of cross section with line scanning mode in the direction perpendicular to the surface. (b) Raman scattering spectra of PVA and *soln*-PVB.

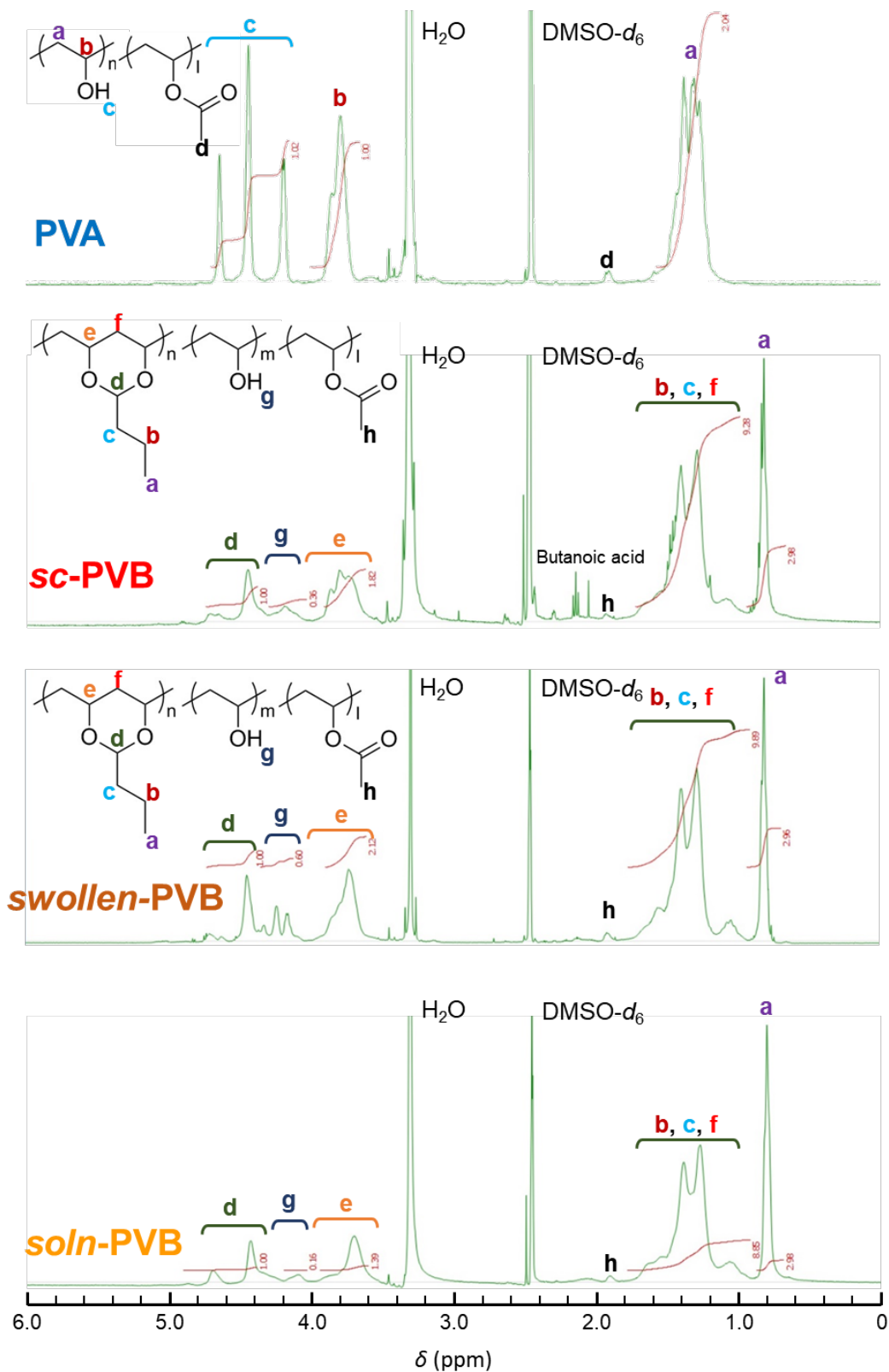


Figure S3. ^1H NMR charts of PVA, *sc*-PVB, *swollen*-PVB and *soln*-PVB in DMSO- d_6 .

Table S1. Acetalization degree of *sc*-PVB, *swollen*-PVB and *soln*-PVB calculated by ^1H NMR measurement.

Sample	Peak area of CH_2	Peak area of CH_3	Mole fraction of vinyl butyral (VB) mol%	Acetalization degree mol%
<i>sc</i> -PVB	9.28	2.98	59.8	74.8
<i>swollen</i> -PVB	9.89	2.96	49.7	66.4
<i>soln</i> -PVB	8.85	2.98	68.7	81.4

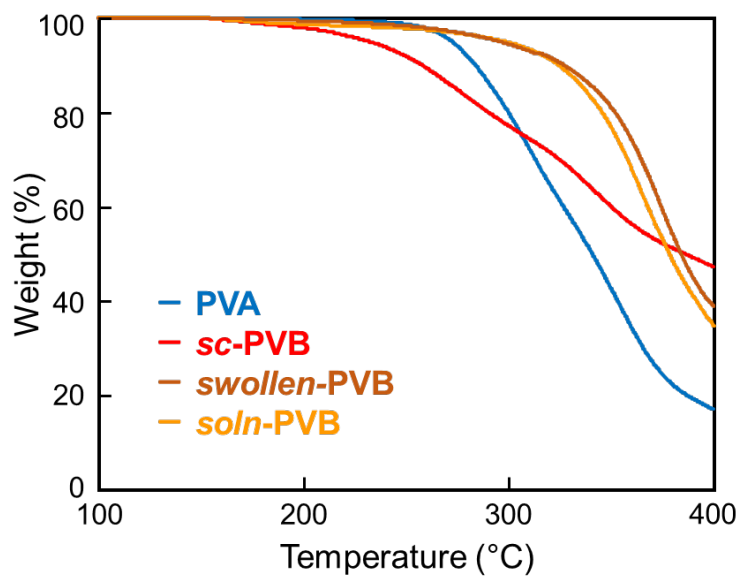


Figure S4. Thermogravimetric trace curves of PVA, *sc*-PVB, *swollen*-PVB and *soln*-PVB.

Table S2. Thermal properties of PVA, *sc*-PVB, *swollen*-PVB and *soln*-PVB.

Sample	T_{d5}	T_g	T_m	X_c
	°C			%
PVA	273	77 ^a	225	46
<i>sc</i> -PVB	231	64	(196) ^b	8.8
<i>swollen</i> -PVB	296	67	(202) ^b	0
<i>soln</i> -PVB	297	56	n.d.	n.d.

^a Measured with 2nd cycle in DSC measurement.

^b Obtained as broad and weak endothermic peaks.

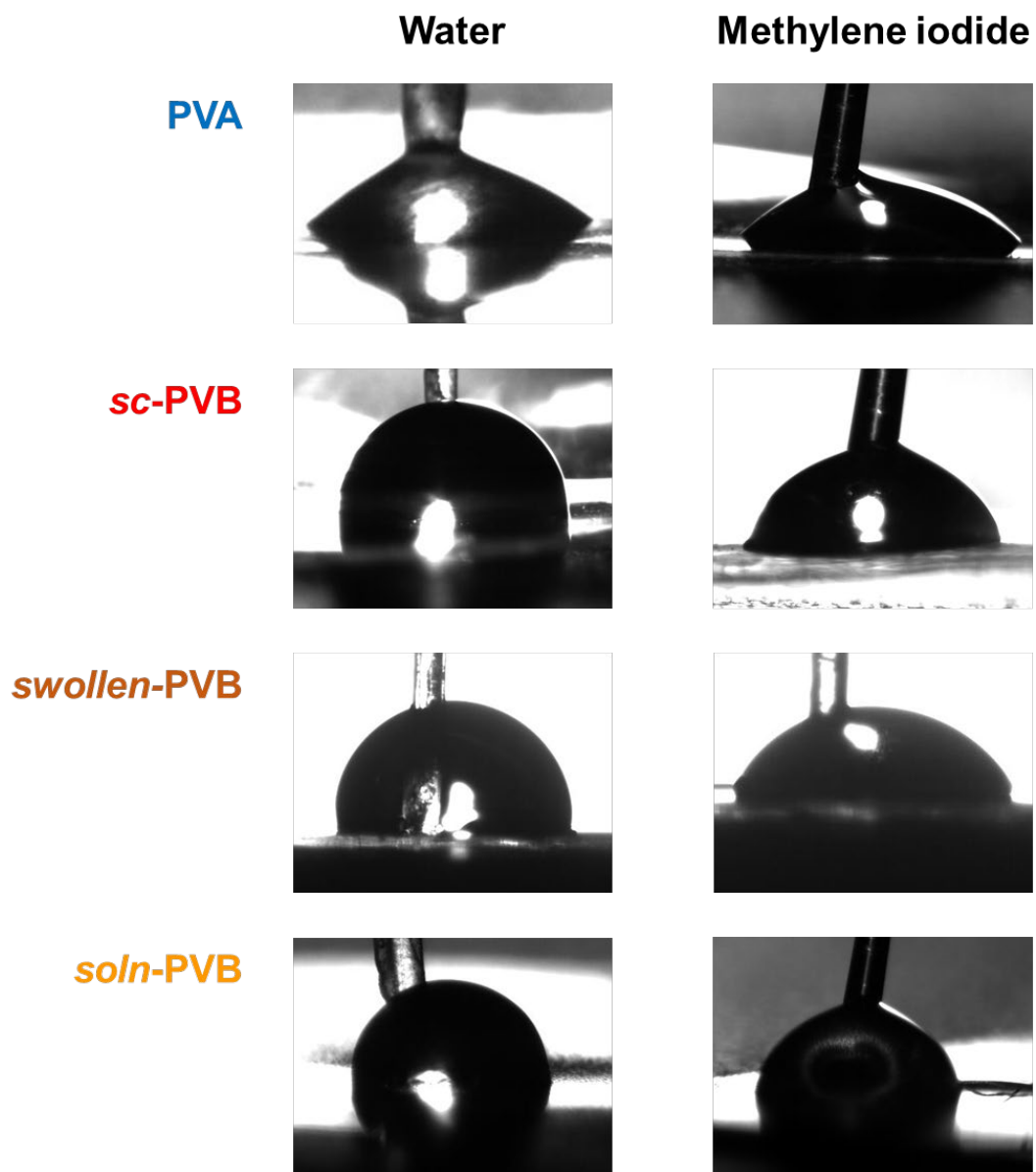


Figure S5. Photograph of droplets of water and methylene iodide on PVA, *sc*-PVB, *swollen*-PVB and *soln*-PVB in measurement of their dynamic contact angles.

Table S3. Mechanical properties of PVA, *sc*-PVB, *swollen*-PVB and *soln*-PVB films.

Sample	Young's modulus	Tensile strength	Elongation at break
	GPa	MPa	%
PVA	5.0±0.5	104±11	44±14
<i>sc</i> -PVB	2.9±0.5	83±7.8	37±7.1
<i>swollen</i> -PVB	1.0±0.3	35±4.8	134±21
<i>soln</i> -PVB	0.028±0.0047	14±2.7	240±40

Table S4. Degree of swelling and ratios of absorbed water of PVA, *sc*-PVB, *swollen*-PVB and *soln*-PVB films with water for 2 h at room temperature.

Sample	Degree of swelling ^a	Ratio of absorbed water
	cm ² /cm ²	g/g
PVA	1.59±0.08	1.60±0.11
<i>sc</i> -PVB	1.01±0.02	0.04±0.03
<i>swollen</i> -PVB	1.05±0.00	0.07±0.03
<i>soln</i> -PVB	1.02±0.01	0.03±0.02

^a (Degree of swelling) = (Area of film after swelling) / (Area of film before swelling)

^b (Ratio of absorbed water) = {(Weight of film after swelling) – (Area of film before swelling)} / (Area of film before swelling)